Efficacy and Safety of ^{124}I-MIBG Dosimetry-Guided High-Activity ^{131}I-MIBG Therapy of Advanced Pheochromocytoma or Neuroblastoma

Ines Maric[1,2], Manuel Weber[1,2], Andre Prochnow[1], Jochen Schmitz[1,2], Nicole Unger[2,3], Benedikt M. Schaarschmidt[2,4], Thorsten D. Poeppel[5], Christoph Rischpler[1,2], Andreas Bockisch[1,2], Ken Herrmann[1,2], Walter Jentzen[1,2], and Wolfgang P. Fendler[1,2]

[1]Department of Nuclear Medicine, University Hospital Essen, University Duisburg-Essen, Essen, Germany; [2]German Cancer Consortium (DKTK), partner site, Essen, Germany; [3]Department of Endocrinology, Diabetes and Metabolism, University Hospital Essen, University Duisburg-Essen, Essen, Germany; [4]Institute of Diagnostic and Interventional Radiology and Neuroradiology, University Hospital Essen, University Duisburg-Essen, Essen, Germany; and [5]Nuklearmedizin, MVZ CDT Strahleninstitut, Cologne, Germany

We aim to evaluate the efficacy and safety of ^{124}I-metaiodobenzylguanidine (MIBG) dosimetry-guided high-activity ^{131}I-MIBG therapy of advanced pheochromocytoma or neuroblastoma. **Methods:** Fourteen patients with advanced pheochromocytoma or neuroblastoma, age 9–69 y, underwent ^{124}I-MIBG PET scans and whole-body retention measurements to assess the whole-body dose as a surrogate of bone marrow toxicity and tumor (absorbed) dose per unit of administered activity. Dosimetry results together with individual patient characteristics were combined to guide a single therapeutic activity to achieve a high tumor dose without exceeding toxicity threshold. Toxicity was assessed for hematologic, hepatic, and renal function. Response was evaluated by RECIST, International Society of Pediatric Oncology Europe Neuroblastoma–like score, change in PET uptake, and quantitative PET parameters (SUV_{max}, SUV_{peak}, metabolic tumor volume, total lesion glycolysis), as well as visual decrease in number or in visual intensity of lesions on baseline to follow-up ^{124}I-MIBG PET/CT. **Results:** The average therapeutic activity was 14 GBq. Eleven of 14 patients (79%) received each more than 10 GBq. One male patient was treated with a single activity of 50 GBq. Three patients were treated with lower activities between 3.5 and 7.0 GBq. Median overall survival was 85 mo (95% CI), and median progression-free survival was 25 mo (95% CI). Four (29%) and 5 (36%) patients demonstrated response (complete response or partial response) by RECIST and functional imaging, respectively. One patient exceeded whole-body dose of 2 Gy and demonstrated grade 3 hematologic toxicity, which resolved spontaneously within 12 mo after the therapy without the need for further treatment. Three patients (21%) demonstrated transient grade 1 renal toxicity. **Conclusion:** ^{124}I-MIBG dosimetry-guided high-activity ^{131}I-MIBG therapy in patients with advanced pheochromocytoma or neuroblastoma resulted in durable responses with a low rate of manageable adverse events. Efficacy of ^{124}I-MIBG–guided activity escalation should further be assessed in a prospective setting.

Key Words: MIBG; therapy; dosimetry; theranostics

J Nucl Med 2023; 64:885–891
DOI: 10.2967/jnumed.122.264775

Received Aug. 15, 2022; revision accepted Jan. 30, 2023.
For correspondence or reprints, contact Ines Maric (ines.maric@uk-essen.de).
Published online Feb. 2, 2023.

Metaiodobenzylguanidine (MIBG), a guanethidine derivative, is a substrate for norepinephrine reuptake transporters, which are highly expressed on the cell surface of neuroendocrine tumors, such as pheochromocytoma or neuroblastoma (*1*). $^{123/131}$I-MIBG imaging is one of the most sensitive lesion detection modalities for pheochromocytoma and neuroblastoma. Although ^{123}I-MIBG allows for quantification, ^{124}I-MIBG offers the benefit of quantification at higher PET spatial resolution (*2,3*). Similar biodistribution compared with ^{123}I-MIBG allows for translation of established systems of image interpretation and therapy monitoring (e.g., International Society of Pediatric Oncology Europe Neuroblastoma score [SIOPEN] or Curie score) (*3–5*). ^{124}I-MIBG imaging and dosimetry is a companion tool for planning of high-activity ^{131}I-MIBG therapy (*6*).

Patients with malignant unresectable, metastatic, or recurring pheochromocytoma have a poor prognosis with an average 5-y survival rate of 12%–20% (*7,8*), whereas in refractory or relapsing neuroblastoma, the 10-y survival probability is less than 15% (*9*). Efficacy of ^{131}I-MIBG for the treatment of unresectable, locally advanced, and metastatic pheochromocytoma and paraganglioma using empiric activities led to recent US Food and Drug Administration approval (*10*). In the prospective trial, objective tumor response occurred in 15 patients (22%; 95% CI, 14%–33%). However, most patients did not demonstrate notable tumor shrinkage despite focal ^{131}I-MIBG uptake in tumor lesions. Nonresponder patients under empiric activities might benefit from high-activity regimens. Pretherapeutic ^{124}I-MIBG PET/CT-based dosimetry of the tumor and organs at risk enables planning of patient-specific activity escalation (*11,12*). However, feasibility, toxicity, and efficacy have, to the authors' knowledge, not yet been assessed.

The aim of this study was to evaluate the efficacy and safety of ^{124}I-MIBG dosimetry-guided high-activity ^{131}I-MIBG therapy in patients with long follow-up after treatment of advanced pheochromocytoma or neuroblastoma.

MATERIALS AND METHODS

Study Design

This is a retrospective, single center study of the efficacy and safety of ^{124}I-MIBG dosimetry-guided, activity-escalated ^{131}I-MIBG therapy of unresectable neural crest tumors. The goal was to achieve a high

tumor (absorbed) dose without exceeding the toxicity threshold. This retrospective analysis was approved by the ethics committee of the University Hospital Essen (reference no. 20–9656-BO). Long-term follow-up included survival, imaging, clinical information, and laboratory data. Primary endpoints in these patients were overall survival (OS) and progression-free survival (PFS) after ^{131}I-MIBG therapy. Secondary endpoints included late hematologic/liver/renal toxicity in relation to the estimated whole-body dose evaluated up to 12 mo after therapy and the efficacy of ^{124}I-MIBG-guided ^{131}1-MIBG therapy as determined by response rate (partial response [PR] and complete response [CR]) within 12 mo after therapy in relation to achieved lesion tumor doses.

Patient Cohort

Patients who underwent ^{124}I-MIBG PET/CT with subsequent ^{131}I-MIBG therapy between August 2006 and July 2016 were included. Thirty patients with histologically proven unresectable neural crest tumors were considered for evaluation. Pretherapeutic imaging revealed no detectable tumor lesions by means of ^{124}I-PET/CT in 16 patients. In total, 14 patients with at least 1 tumor lesion with measurable volume and uptake underwent tumor and whole-body dosimetry. All therapy patients demonstrated progressive disease at baseline, defined either by an endocrinologist/oncologist by worsening clinical symptoms or by radiology/nuclear medicine specialists, defined by RECIST, or both. All patients received a potassium iodide–saturated solution to prevent thyroid accumulation of free radioactive iodine starting 48 h before administration and continuing for 15 d after therapy according to European Association of Nuclear Medicine Practice Guidelines (*13*). The patients provided written informed consent before dosimetry and therapy and were admitted to our ward in accordance with radiation protection requirements. Both ^{124}I- and ^{131}I-MIBG were applied intravenously. Labeling and preparation of the carrier-added ^{124}I-MIBG are described elsewhere (*3*).

Tumor and Whole-Body Dosimetry

Our ^{124}I-MIBG dosimetry protocol involves determination of the estimated tumor dose per unit of administered ^{131}I-MIBG activity for selected tumor deposits by serial PET and PET/CT examinations (*14*) and of determination of the maximum tolerable whole-body ^{131}I-MIBG activity via whole-body retention measurements (*11*). The approach is similar to the pretherapy dosimetry protocol used in thyroid cancer patients (*15–17*). Both the tumor dose and maximum tolerable whole-body ^{131}I-MIBG activity serve as primary input for the choice of the actual recommended therapeutic activity and other interventions, supplemented by clinical judgment based on patient and disease characteristics (age, previous myelotoxic therapies, current general and nutritional condition, comorbidities, notes from [pediatric] oncologists, availability of autologous stem cells) and biochemistry results (bone marrow and kidney and liver function).

For tumor dosimetry, serial PET data were acquired 4, 24, 48, and 96–120 h after ^{124}I-MIBG administration (average activity of 46 MBq

TABLE 1
Patient Characteristics

Characteristic (n = 14)	Patient			
	n	%	Median	Range
Diagnosis				
Pheochromocytoma	10	(71)		
Neuroblastoma	4	(29)		
Sex				
Male	8	(57)		
Female	6	(43)		
Age at entry (y)			36	9–69
Time from diagnosis to entry (mo)			66	1–189
Prior treatments				
Surgery	13	(93)		
Radiotherapy	6	(43)		
Chemotherapy	7	(50)		
No. of ^{131}I-MIBG therapies				
1	14	(100)		
2	8	(57)		
3	2	(14)		
4	1	(7)		
5	1	(7)		
^{131}I-MIBG activity at entry (GBq)			10.5	3.5–50
^{131}I-MIBG activity, all treatments (GBq)			38	4.8–50
TNM				
N1	9	(64)		
M1 bone	8	(57)		
M1 visceral	9	(64)		

^{124}I-MIBG). The PET scans were performed on 2 PET systems: a dedicated ECAT EXACT HR+ PET scanner (Siemens) and a PET/CT Biograph Emotion Duo scanner (Siemens Medical Solutions). The interscanner variability was examined elsewhere (*18*), demonstrating good agreement between the 2 systems with individual deviations of less than 10%. PET and PET/CT emission data were acquired through whole-body scans performed from head to thigh using 5–8 bed positions (5 min each). PET image reconstruction was performed using an iterative attenuation-weighted ordered-subset expectation maximation algorithm (2 iterations and 8 subsets, 5-mm postreconstruction gaussian filter) (*17*). For the dedicated PET and PET/CT scanning, the rod source transmission data and CT data were used for PET attenuation correction, respectively. Recovery correction was performed as described by Jentzen et al. (*14*). The metastatic lesion volumes for recovery correction were estimated using anatomic information obtained by the CT component of PET/CT. If no lesion volume could be derived from anatomic information, a PET volumetric segmentation method was used (*19,20*). The predicted cumulative activity per unit of administered ^{131}I-MIBG activity (tumor residence time) was obtained using the time–activity curves of the serial PET scans corrected with the measured recovery coefficient and corrected for the difference in the physical half-lives of ^{124}I and ^{131}I (*14,21*). Both the tumor volume (mass) and the respective residence time were used to predict the tumor dose using the sphere model of OLINDA/EXM.

For whole-body dosimetry, multiple whole-body retention measurements (2, 4, 24, 48, 72, and 96 h after ^{124}I-MIBG administration) were performed placing the patient approximately 3 m in front of an uncollimated γ-camera (E.CAM Signature Series; Siemens). Anterior and posterior counts for calculation of a geometric mean were measured considering dead time effects. After correcting for the difference in the physical half-lives of ^{124}I and ^{131}I, the whole-body residence time was calculated using the whole-body retention curves. The predicted whole-body dose per unit administered activity was calculated using the whole-body-to-whole-body S values corrected for patient mass (*11*). The resulting whole-body dose per administered activity was used to calculate the maximum tolerable whole-body ^{131}I-MIBG activity, a value that represents the maximum therapeutic activity that can be safely administered without exceeding the 2-Gy whole-body absorbed dose threshold (as a surrogate to estimate the myelotoxicity).

Analysis

At least 1 and up to 4 tumor lesions with measurable volume and uptake were taken into consideration per patient. Toxicity was graded with Common Terminology Criteria for Adverse Events version 3.0. Response was evaluated by baseline to follow-up changes in ^{124}I-MIBG-PET/CT, defined by RECIST criteria (*10*), and by visual and quantitative (SUV_{max}, SUV_{peak}, metabolic tumor volume, total lesion glycolysis) PET analysis. For tumors in which exact size measurements were not available, such as osteoblastic bone metastases, a visual impression of nuclear medicine physicians was used. Visual ^{124}I-MIBG PET evaluation was categorized as follows: CR was described as the disappearance of all lesions; PR was a decrease in the number or visual intensity of lesions; stable disease was no discernible change; and progressive disease was the appearance of new lesions (*11*). Furthermore, we defined a SIOPEN-like score for baseline to follow-up response assessment (not including the assessment of soft-tissue areas of tumor) as follows: the scan area was segmented into 8 body regions, excluding the 4 lower limb areas, which are not included in the usual PET/CT scan field of view performed in the clinical routine in our institution. Each region was assigned with 1–6 points, corresponding to established SIOPEN scoring (*4*), and then summarized. The baseline to follow-up change in this sum was then used as an additional mean to assess the response in accordance with the SIOPEN score.

Statistics and Software

Statistical analysis was performed using IBM SPSS Statistics, version 26 (IBM Corp.). Patient characteristics, toxicity, and response are presented as descriptive statistics. Assessment of statistically significant differences between groups was performed using a *t* test. Predictors for PFS and OS were assessed by univariate Cox regression analysis and log-rank test and plotted using Kaplan–Meier curves. PMOD 3.1 (PMOD Technologies Ltd.) was used to coregister and determine the volumes and activities shown. The absorbed tumor dose was calculated using OLINDA/EXM 1.1 software (Vanderbilt University).

RESULTS

Patient Characteristics

Patient characteristics are summarized in Table 1. The mean patient age (range) was 36 (9–69) y. Six of 14 (43%) patients were female, and 8 of 14 (57%) were male. Among the 14 patients, 4 (29%) had histologically confirmed neuroblastoma and 10 (71%) had malignant pheochromocytoma. An average time period of 1.2 ± 1.6 (SD) mo from pretherapeutic ^{124}I-MIBG dosimetry to therapy and an average of 4.6 ± 2.4 (SD) mo for the interval between therapy and posttherapeutic follow-up PET/CT were documented. A single therapy activity ranged from 3.5 to 50 GBq

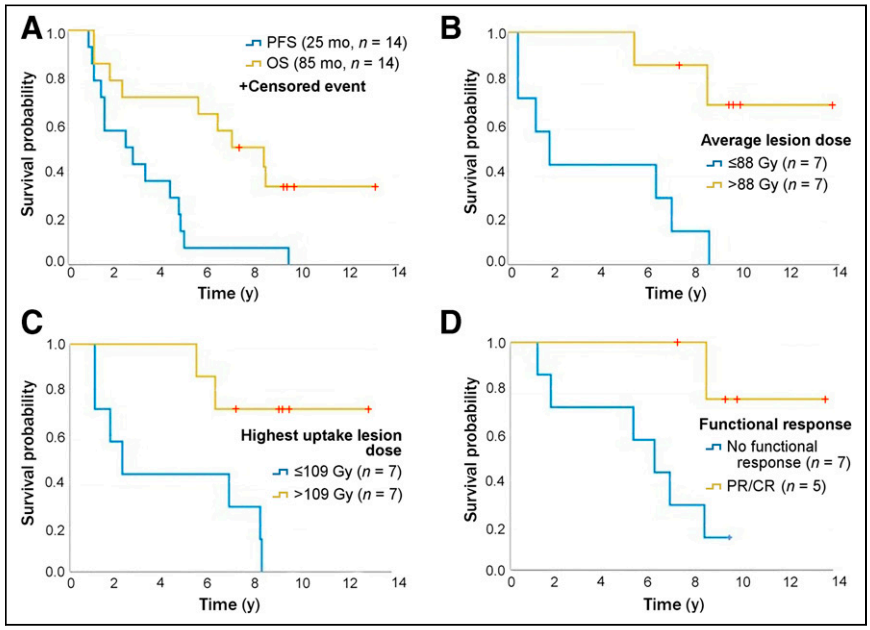

FIGURE 1. Kaplan–Meier survival. (A) OS and PFS of patients who underwent ^{124}I-MIBG PET-based dosimetry followed by ^{131}I-MIBG therapy; OS was significantly associated with several factors, including (B) average tumor lesion dose higher than median (88 Gy; $P < 0.004$); (C) highest uptake tumor lesion dose higher than median (109 Gy; $P < 0.009$); and (D) functional response as assessed by ^{124}I-MIBG PET/CT ($P < 0.001$). Predictors for PFS and OS were assessed by univariate Cox regression analysis and log-rank test and plotted using Kaplan–Meier curves.

TABLE 2
Dosimetry Data of Patients Who Underwent ^{124}I-MIBG PET-Based Dosimetry Followed by Targeted ^{131}I-MIBG Therapy

Characteristic (n = 14)	Patient
Whole-body dose (Gy)	
Median	1.45
Range	0.48–6

(average, 13.7 GBq; ±11.3 SD). The average time from diagnosis to dosimetry-based ^{131}I-MIBG therapy was 75 ± 55.8 (SD) mo (range, 1–189 mo). All eligible patients had received previous therapies, including surgery (93%), radiotherapy (43%), or chemotherapy (50%).

Survival

Figure 1 shows OS and PFS along with predictors of survival.

Median OS after therapy was 85 mo (hazard ratio 6.9; 95% CI [3.2–10.5]), and median PFS was 25 mo (hazard ratio 1.9; 95% CI [0.0–4.3]). Minimum follow-up time was 5 mo, and the average follow-up time (range) for the cohort was 76 ± 48.7 (SD) mo (range, 5–164 mo). Five of 14 (36%) patients died during the observation period. By log-rank analysis, significant predictors of OS and functional response were achieved with average tumor lesion dose higher than median (88 Gy; $P < 0.004$), the highest uptake lesion dose higher than median (109 Gy; $P < 0.009$), and the functional response by means of ^{124}I-MIBG PET/CT defined as CR/PR, respectively ($P < 0.001$). Changes in SIOPEN-like score translated from conventional ^{123}I-MIBG imaging did not show a significant correlation with OS ($P < 0.205$) or response ($P < 0.059$ for morphologic response and $P < 0.017$ for functional response).

Dosimetry and Toxicity

The dosimetry and toxicity data are shown in Tables 2 and 3. One patient received a single therapy activity of 50 GBq ^{131}I-MIBG (in a curative intention and close cooperation with the pediatric oncologists, after autologous stem cells have been collected and cryopreserved), exceeded the estimated whole-body dose of 2 Gy (median in all patients, 1.4 Gy; range, 0.4–6 Gy), and demonstrated transient grade 3 hematologic toxicity (leukocytopenia and thrombocytopenia), which resolved spontaneously within 12 mo after therapy without the need for stem cell rescue. Additionally, 2 patients demonstrated grade 1 hematologic toxicity. Transitional grade 1 kidney function deterioration was noted in 3 patients (21%). One patient with pheochromocytoma showed a transitional grade 1 kidney function deterioration after receiving a cumulative activity of 21.6 GBq and was diagnosed with operable urothelial carcinoma (pTa, R0) 4 y after ^{131}I-MIBG therapy.

TABLE 3
Toxicity Data of Patients (n = 14) Who Underwent ^{124}I-MIBG PET-Based Dosimetry Followed by Targeted ^{131}I-MIBG Therapy

	Any grade		Grades 3–4	
Category	n	%	n	%
Hematologic	3	21	1	7
Renal	3	21	0	0
Possible secondary malignancy	1	7	Urothelial carcinoma	

Treatment Response

Treatment response is summarized in Table 4. Of the 14 evaluable patients, 4 (29%) and 5 (36%) demonstrated CR/PR by RECIST and functional imaging, respectively. Disease control, defined by CR, PR, or stable disease, was achieved in 71% of the patients according to morphologic imaging and in 79% by functional imaging. All 4 patients (3 with neuroblastoma and 1 with metastatic pheochromocytoma) demonstrating progressive disease by means of morphologic imaging were extensively pretreated during the long disease history.

The median tumor dose of the lesions with highest uptake was 109 Gy, ranging from 10.5 to 495 Gy. An overview of individual patient characteristics combined with individual tumor dose along with response is given in Table 5. Figure 2 shows an example of a patient with metastatic pheochromocytoma. Figure 3 shows an example of a patient with metastatic neuroblastoma.

DISCUSSION

^{131}I-MIBG is an efficacious therapy for MIBG-positive unresectable, locally advanced/metastatic neural crest tumors. Prospective phase 2 data (*10*) recently led to the US Food and Drug Administration approval of ^{131}I-MIBG for the treatment of unresectable, locally advanced, and metastatic pheochromocytoma and paraganglioma using empiric activities. High-activity ^{131}I-MIBG therapy has been reported previously; however, the feasibility of the $^{124/131}$I-MIBG theranostic pair for dose escalation has not yet been assessed systematically. Here we demonstrate feasibility of dosimetry guided $^{124/131}$I-MIBG theranostic therapy, which resulted in durable responses in 57% and 50% of patients at 12 and 24 mo, respectively. Median OS after therapy was 85 mo, and median PFS was 25 mo, which compares favorably to previously published data (*10,22,23*). For instance, overall response (CR/PR) rate was 22%, and 8% of patients maintained stable disease for greater than 12 mo in the cohort described by Gonias et al. (*22*). In comparison, the median OS was 36.7 mo in a study by Pryma et al. (*10*). In the long-term follow-up, 1 grade 3 event was noted for 1 patient, and possible secondary malignancy

TABLE 4
Morphologic (CT/MRI) and Functional (PET) Response After ^{131}I-MIBG Therapy (n = 14)

	(RECIST) CT/MRI		^{124}I-MIBG PET	
Response	n	%	n	%
CR	0	0	0	0
PR	4	29	5	36
Stable disease	6	43	6	43
PD	4	29	1	7
No follow-up	0	0	2	14
Disease control (CR, PR, stable disease)	10	71	11	79
Any response (CR, PR)	4	29	5	36

TABLE 5
Individual Patient Characteristics Combined with Tumor Dose and Response

Patient characteristic (n=14)	Patient													
	1	2	3	4	5	6	7	8	9	10	11	12	13	14
Sex	M	F	F	M	M	F	M	M	F	M	M	M	F	F
Age at entry, y	17	24	68	69	57	23	54	65	68	38	34	9	21	16
Diagnosis	PCC	PCC	PCC	PCC	PCC	PCC	PCC	PCC	PCC	PCC	NB	NB	NB	NB
N1	Yes	No	Yes	No	Yes	Yes	No	Yes	No	Yes	Yes	No	Yes	Yes
M1	Yes	Yes	Yes	Yes	Yes	No	Yes	Yes	Yes	Yes	Yes	Yes	Yes	Yes
Time from diagnosis to entry, mo	7	1	122	3	101	50	144	51	79	79	189	53	123	53
^{131}I-MIBG activity, GBq	50.0	15.0	10.0	7.0	10.0	20.0	15.0	3.5	10.0	11.0	10.0	4.8	11.0	15.0
Number of MIBG therapies	1	1	5	2	2	2	1	2	2	1	2	1	3	1
Activity (all) MIBG therapies, GBq	50.0	15.0	38.0	21.6	21.1	27.4	15.0	10.5	20.0	11.0	16.0	4.8	26.2	15.0
Whole-body dose after therapy, Gy	6.0	1.8	1.4	0.5	1.3	2.0	1.7	1.1	1.7	1.5	0.9	0.5	1.0	1.5
Median absorbed tumor dose, Gy	356.5	93.0	78.0	93.1	208.5	107.0	40.5	10.5	179.0	41.8	142.8	9.0	30.8	82.5
Number of prior therapy lines	1	1	2	2	3	1	3	2	1	1	5	3	4	3
Chemotherapy/radiation	Yes	No	No	No	Yes	No	Yes	No	No	No	Yes	Yes	Yes	Yes
Surgery	No	Yes	Yes	Yes	Yes	Yes	Yes	Yes	Yes	Yes	Yes	Yes	Yes	Yes
Time from dosimetry to therapy, mo	0	0	1	1	0	2	2	1	1	0	0	6	3	0
Time from therapy to dosimetry follow-up, mo	3	6	7	11	6	3	4	3	3	5	4	1	5	4
OS, mo	164	112	75	101	118	114	14	21	87	83	64	5	102	5
PFS, mo	115	48	27	11	53	54	11	9	34	5	23	2	56	4
Morphologic response	Stable disease	PR	PD	PR	Stable disease	Stable disease	Stable disease	PD	Stable disease	Stable disease	PD	PD	PD	PR
Functional response	PR	PR	PR	PR	Stable disease	Stable disease	Stable disease	PD	Stable disease	Stable disease	NA	Stable disease	NA	PR
SIOPEN-like score (baseline)	11	5	17	8	5	16	4	6	6	39	39	6	20	9
SIOPEN-like score (follow up)	11	4	7	7	4	11	4	6	6	32	NA	6	NA	7

Morphologic response was determined by RECIST (PR, lesion diameter decreasing in 30%; PD, lesions diameter increasing in 20% or appearance of new lesions; stable disease, none of the aforementioned criteria are met); functional response was assessed as change in baseline to follow-up ^{124}I-MIBG imaging (PR, decrease in lesion number/uptake intensity; stable disease, no significant change; PD, new lesions). The change in SIOPEN-like score was consistent with outcome; however, it was not statistically significant.

PCC = pheochromocytoma; NB = neuroblastoma. NA = not available.

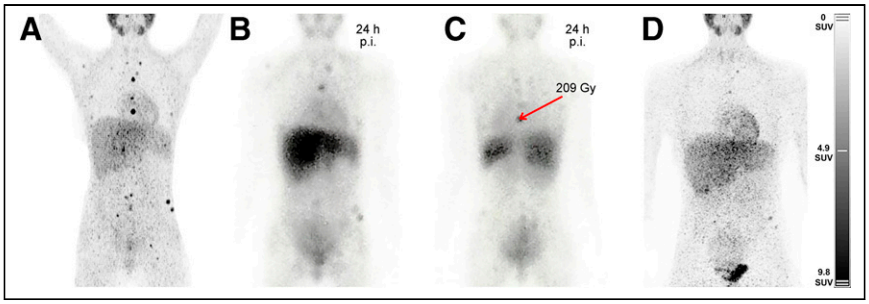

FIGURE 2. Patient 2 (female, 24 y) with metastatic pheochromocytoma before (A) and 6 mo after (D) single ^{124}I-MIBG dosimetry-guided high-activity ^{131}I-MIBG therapy with 15 GBq (B and C: post-therapeutic scintigraphy 24 h after injection, anterior and posterior views). PR in morphologic and functional imaging was noted 6 mo after treatment (OS was 112 mo and PFS was 48 mo; maximum lesion dose [marked with arrow] achieved was 209 Gy). p.i. = after injection.

was noted in 1 patient in our cohort. The much lower toxicity rates compared with previous data, reporting grade 3/4 neutropenia in 85%, low platelet count in 83%, and anemia in 8% of patients (*22*), additionally strengthen ^{124}I-MIBG dosimetry to mitigate toxicity.

This study demonstrates the advantages of calculated treatment planning and targeted therapy in a heterogenous group of patients with neural crest tumors. Here we provide evidence for the feasibility of using the theranostic pair ^{124}I/^{131}I-MIBG to achieve a high tumor dose without exceeding toxicity thresholds, especially for the bone marrow (*10,22*). The superior diagnostic performance and improved possibilities of quantification of ^{124}I-MIBG PET/CT over scintigraphy with ^{123}I- or ^{131}I-MIBG have been discussed and confirmed in the current literature (*2,3,24*). Previous studies conducted in a preclinical environment have shown similar potential (*6,25*). Furthermore, the use of the ^{124}I/^{131}I pair is well established for imaging and therapy of differentiated thyroid carcinoma (*15,26–29*).

A low adverse events rate in comparison with other activity-escalated concepts (*22,23,30,31*) additionally confirms the central role of ^{124}I-MIBG PET/CT dosimetry in targeted therapy planning. Improved quantification possibilities using ^{124}I-MIBG PET/CT and the knowledge of tumor doses can further help to assess the individual response probability and establish the threshold doses needed to achieve partial or complete response (absorbed doses in relation to associated response rates), similar to data published for differentiated thyroid carcinoma (*26,32–34*). Significant predictors of OS and functional response in our cohort were an achieved tumor dose in the highest uptake lesion higher than 109 Gy and the average achieved dose higher than 88 Gy, as well as the functional response defined as CR/PR. Disease control, defined by either CR, PR, or stable disease, was achieved in 71% of the patients by morphologic imaging and in 79% by functional imaging lesion count, respectively. Changes in SIOPEN-like score did not show a significant correlation with OS or response. An association between lesions dose and response/survival is noted. Therefore, dosimetry-guided high-activity therapy could be critical for favorable outcomes. In addition, through ^{124}I-MIBG prescreening/dosimetry, patients most likely to benefit from ^{131}I-MIBG therapy can be selected, and long-term outcomes can be predicted to guide subsequent management.

Strengths of our study include dosimetry guidance and long-term follow-up with mature survival data. Limitations of this study include a small sample size, the retrospective study design, and the heterogenous patient cohort concerning tumor entity and age. Prospective studies are needed to compare efficacy and safety of ^{124}I-MIBG dosimetry-guided ^{131}I-MIBG therapy versus conventional ^{131}I-MIBG therapy using standard activities in larger patient cohorts.

CONCLUSION

^{124}I-MIBG dosimetry-guided high-activity ^{131}I-MIBG therapy is feasible and results in durable responses, long survival, and a low rate of manageable adverse events. ^{124}I-MIBG PET-derived tumor dose and response assessment predict survival after ^{131}I-MIBG therapy.

^{124}/^{131}I-MIBG theranostics offer individual treatment planning with a promising efficacy/safety tradeoff: ^{124}I-MIBG–guided ^{131}I-MIBG activity escalation should further be assessed in prospective trials.

DISCLOSURE

This work is a part of the doctoral thesis of Ines Maric. Andre Prochnow, Jochen Schmitz, Nicole Unger, Thorsten Poeppel, Christoph Rischpler and Andreas Bockisch have nothing to declare. Walter Jentzen received research funding from Siemens Healthineers. Manuel Weber reports fees from Boston Scientific, Terumo, Advanced Accelerator Applications, and Lilly, outside of the submitted work. Benedikt M. Schaarschmidt is supported by a research grant from PharmaCept, outside the submitted work. Ken Herrmann reports personal fees from Bayer SIRTEX, Adacap, Curium, Endocyte, IPSEN, Siemens Healthineers, GE Healthcare, Amgen, Novartis, and ymabs; personal fees and other from Sofie Biosciences; nonfinancial support from ABX; and grants and personal fees from BTG, outside the submitted work. Wolfgang Fendler reports fees from SOFIE Bioscience (research funding), Janssen (consultant, speaker), Calyx (consultant), Bayer (consultant, speaker, research

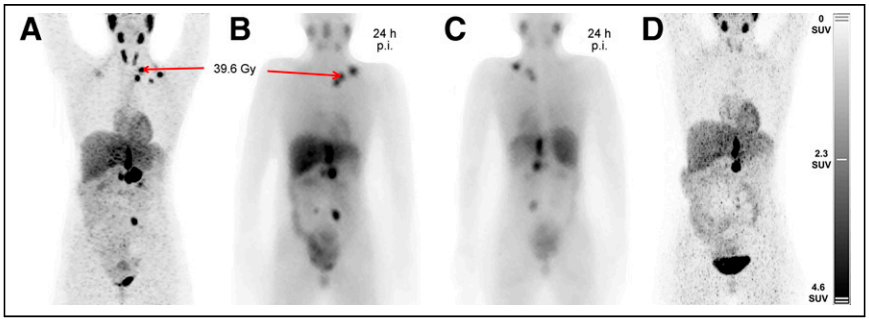

FIGURE 3. Patient 13 (female, 21 y) with metastatic neuroblastoma before (A) and 5 mo after (D) single ^{124}I-MIBG dosimetry-guided high-activity ^{131}I-MIBG therapy with 11 GBq (B and C: posttherapeutic scintigraphy 24 h after injection, anterior and posterior views, respectively). Maximum lesion dose achieved was 39.6 Gy (arrows). PR in morphologic and functional imaging was noted 5 mo after treatment (OS was 102 mo and PFS was 56 mo). p.i. = after injection.

funding), Parexel (image review), Novartis (speaker), and Telix (speaker), outside of the submitted work. No other potential conflict of interest relevant to this article was reported.

KEY POINTS

QUESTION: Is ^{124}I-MIBG dosimetry-guided high-activity ^{131}I-MIBG therapy of advanced pheochromocytoma or neuroblastoma effective and safe?

PERTINENT FINDINGS: ^{124}I-MIBG dosimetry-guided high-activity ^{131}I-MIBG therapy is feasible and results in durable responses, long survival, and a low rate of manageable adverse events. ^{124}I-MIBG PET tumor uptake and tumor response assessment can further predict outcome after ^{131}I-MIBG therapy.

IMPLICATIONS FOR PATIENT CARE: ^{124}/^{131}I-MIBG theranostics offer individual treatment planning with a promising efficacy/safety tradeoff: ^{124}I-MIBG-guided ^{131}I-MIBG activity escalation should further be assessed in prospective trials.

REFERENCES

1. Vallabhajosula S, Nikolopoulou A. Radioiodinated metaiodobenzylguanidine (MIBG): radiochemistry, biology, and pharmacology. *Semin Nucl Med.* 2011;41:324–333.
2. Aboian MS, Huang SY, Hernandez-Pampaloni M, et al. ^{124}I-MIBG PET/CT to monitor metastatic disease in children with relapsed neuroblastoma. *J Nucl Med.* 2021;62:43–47.
3. Weber M, Schmitz J, Maric I, et al. Diagnostic performance of [124 I]m-iodobenzylguanidine PET/CT in patients with pheochromocytoma. *J Nucl Med.* 2022;63:869–874.
4. Lewington V, Lambert B, Poetschger U, et al. ^{123}I-mIBG scintigraphy in neuroblastoma: development of a SIOPEN semi-quantitative reporting, method by an international panel. *Eur J Nucl Med Mol Imaging.* 2017;44:234–241.
5. Ady N, Zucker J, Asselain B, et al. A new ^{123}I-MIBG whole body scan scoring method–application to the prediction of the response of metastases to induction chemotherapy in stage IV neuroblastoma. *Eur J Cancer.* 1995;31A:256–261.
6. Marsh IR, Grudzinski J, Baiu DC, et al. Preclinical pharmacokinetics and dosimetry studies of ^{124}I/^{131}I-CLR1404 for treatment of pediatric solid tumors in murine xenograft models. *J Nucl Med.* 2019;60:1414–1420.
7. John H, Ziegler WH, Hauri D, Jaeger P. Pheochromocytomas: can malignant potential be predicted? *Urology.* 1999;53:679–683.
8. Park J, Song C, Park M, et al. Predictive characteristics of malignant pheochromocytoma. *Korean J Urol.* 2011;52:241–246.
9. Garaventa A, Parodi S, De Bernardi B, et al. Outcome of children with neuroblastoma after progression or relapse. A retrospective study of the Italian neuroblastoma registry. *Eur J Cancer.* 2009;45:2835–2842.
10. Pryma DA, Chin BB, Noto RB, et al. Efficacy and safety of high-specific-activity ^{131}I-MIBG therapy in patients with advanced pheochromocytoma or paraganglioma. *J Nucl Med.* 2019;60:623–630.
11. Buckley SE, Chittenden SJ, Saran FH, Meller ST, Flux GD. Whole-body dosimetry for individualized treatment planning of ^{131}I-MIBG radionuclide therapy for neuroblastoma. *J Nucl Med.* 2009;50:1518–1524.
12. Buckley SE, Saran FH, Gaze MN, et al. Dosimetry for fractionated ^{131}I-mIBG therapies in patients with primary resistant high-risk neuroblastoma: Preliminary results. *Cancer Biother Radiopharm.* 2007;22:105–112.
13. Giammarile F, Chiti A, Lassmann M, Brans B, Flux G. EANM procedure guidelines for ^{131}I-meta-iodobenzylguanidine (^{131}I-mIBG) therapy. *Eur J Nucl Med Mol Imaging.* 2008;35:1039–1047.
14. Jentzen W, Freudenberg L, Bockisch A. Quantitative imaging of (124)I with PET/CT in pretherapy lesion dosimetry. Effects impairing image quantification and their corrections. *Q J Nucl Med Mol Imaging.* 2011;55:21–43.
15. Jentzen W, Bockisch A, Ruhlmann M. Assessment of simplified blood dose protocols for the estimation of the maximum tolerable activity in thyroid cancer patients undergoing radioiodine therapy using ^{124}I. *J Nucl Med.* 2015;56:832–838.
16. Jentzen W, Hoppenbrouwers J, Van Leeuwen P, et al. Assessment of lesion response in the initial radioiodine treatment of differentiated thyroid cancer using ^{124}I PET imaging. *J Nucl Med.* 2014;55:1759–1765.
17. Freudenberg LS, Jentzen W, Görges R, et al. ^{124}I-PET dosimetry in advanced differentiated thyroid cancer: therapeutic impact. *Nucl Med (Stuttg).* 2007;46:121–128.
18. Jentzen W, Weise R, Kupferschläger J, et al. Iodine-124 PET dosimetry in differentiated thyroid cancer: recovery coefficient in 2D and 3D modes for PET(/CT) systems. *Eur J Nucl Med Mol Imaging.* 2008;35:611–623.
19. Jentzen W, Freudenberg L, Eising EG, Heinze M, Brandau W, Bockisch A. Segmentation of PET volumes by iterative image thresholding. *J Nucl Med.* 2007;48:108–114.
20. Jentzen W. An improved iterative thresholding method to delineate PET volumes using the delineation-averaged signal instead of the enclosed maximum signal. *J Nucl Med Technol.* 2015;43:28–35.
21. Jentzen W, Hobbs RF, Stahl A, Knust J, Sgouros G, Bockisch A. Pre-therapeutic ^{124}I PET(/CT) dosimetry confirms low average absorbed doses per administered ^{131}I activity to the salivary glands in radioiodine therapy of differentiated thyroid cancer. *Eur J Nucl Med Mol Imaging.* 2010;37:884–895.
22. Gonias S, Goldsby R, Matthay KK, et al. Phase II study of high-dose [131i]metaiodobenzylguanidine therapy for patients with metastatic pheochromocytoma and paraganglioma. *J Clin Oncol.* 2009;27:4162–4168.
23. Wakabayashi H, Kayano D, Inaki A, et al. High-dose ^{131}I-mIBG as consolidation therapy in pediatric patients with relapsed neuroblastoma and ganglioneuroblastoma: the Japanese experience. *Ann Nucl Med.* 2020;34:840–846.
24. Shapiro B, Copp JE, Sisson JC, Eyre PL, Wallis J, Beierwaltes WH. Iodine-131 metaiodobenzylguanidine for the locating of suspected pheochromocytoma: experience in 400 cases. *J Nucl Med.* 1985;26:576–585.
25. Lee CL, Wahnishe H, Sayre GA, et al. Radiation dose estimation using preclinical imaging with i 124 -metaiodobenzylguanidine (MIBG) PET. *Med Phys.* 2010;37:4861–4867.
26. Jentzen W, Freudenberg L, Eising EG, Sonnenschein W, Knust J, Bockisch A. Optimized ^{124}I PET dosimetry protocol for radioiodine therapy of differentiated thyroid cancer. *J Nucl Med.* 2008;49:1017–1023.
27. Kolbert KS, Pentlow KS, Pearson JR, et al. Prediction of absorbed dose to normal organs in thyroid cancer patients treated with ^{131}I by use of ^{124}I PET and 3-dimensional internal dosimetry software. *J Nucl Med.* 2007;48:143–149.
28. Ruhlmann M, Sonnenschein W, Nagarajah J, Binse I, Herrmann K, Jentzen W. Pretherapeutic 124 i dosimetry reliably predicts intratherapeutic blood kinetics of 131 i in patients with differentiated thyroid carcinoma receiving high therapeutic activities. *Nucl Med Commun.* 2018;39:457–464.
29. Ballinger JR. Theranostic radiopharmaceuticals: established agents in current use. *Br J Radiol.* 2018;91:20170969.
30. Rubio PM, Galán V, Rodado S, Plaza D, Martínez L. MIBG therapy for neuroblastoma: precision achieved with dosimetry, and concern for false responders. *Front Med (Lausanne).* 2020;7:173.
31. Weiss B, Vora A, Huberty J, Hawkins RA, Matthay KK. Secondary myelodysplastic syndrome and leukemia following ^{131}I-metaiodobenzylguanidine therapy for relapsed neuroblastoma. *J Pediatr Hematol Oncol.* 2003;25:543–547.
32. Maxon HR, Englaro EE, Thomas SR, et al. Radioiodine-131 therapy for well-differentiated thyroid cancer—a quantitative radiation dosimetric approach: outcome and validation in 85 patients. *J Nucl Med.* 1992;33:1132–1136.
33. Jentzen W, Verschure F, Van Zon A, et al. ^{124}I PET assessment of response of bone metastases to initial radioiodine treatment of differentiated thyroid cancer. *J Nucl Med.* 2016;57:1499–1504.
34. Wierts R, Brans B, Havekes B, et al. Dose-response relationship in differentiated thyroid cancer patients undergoing radioiodine treatment assessed by means of ^{124}I PET/CT. *J Nucl Med.* 2016;57:1027–1032.